Master of
Science Thesis
VT2019

New potential treatment protocol for radiotherapy of glioblastoma

---

Victor Pham

Supervision

Jonas Scherman, Per Munck af Rosenschöld, Michael Lundemann, Daniel Gasic and Søren Møller

Department of Medical Radiation Physics,
Clinical Sciences, Lund
Lund University

Popular scientific summary in Swedish

Under de senaste decennierna har antalet diagnostiserade cancerfall stadigt ökat. För patienter med den ödesdigra hjärntumören glioblastom har överlevnadsstatistiken dock stått still. Forskare i Lund och Köpenhamn tros nu ha funnit pusselbiten som kan komma att ändra på detta.

Cancern är en av de dödligaste sjukdomarna i Sverige och stod för 26 procent av alla dödsfall år 2017. Däremot har man under de senaste 30–40 åren lyckats att nästan fördubbla antalet patienter som är vid liv tio år efter sin cancerdiagnos. Bättre teknik och förståelse för sjukdomarna har lett till att flera cancertyper, inklusive de två allra vanligaste, idag har relativt god överlevnadsstatistik. En cancertyp vars prognos inte är så god är hjärncancern glioblastom. Lyckligtvis hör hjärntumörerna till de ovanligare typerna av cancertumörer, eftersom de flesta glioblastompatienter avlider inom två år. Utan behandling tar det endast någon månad. Anledningen är att cancercellerna tycks vara resistenta mot dagens behandling, vilken består av att man först kirurgiskt försöker avlägsna så mycket som möjligt av tumören, följt av chemo- och strålterapi. Tråkigt nog tenderar tumören att komma tillbaka (det kallas då för recidiv) till området som har behandlats, endast månader efter avslutad behandling.
Strålning förknippas i samhället idag som något otäckt, då trots att den inte syns eller känns kan orsaka förödande konsekvenser. Om man däremot använder den rätt kan den komma till oerhörd nytta. Hälften av alla cancerpatienter idag genomgår strålterapi. Genom att fokusera strålningen mot tumören kan man ta kål på tumörcellerna. Haken med strålbehandlingar är dock att stora delar frisk vävnad oundvikligen också bestrålas, om än i lägre utsträckning.

Man har nyligen sett att det finns en stark korrelation mellan hög medelstråldos till hela hjärnan och sämre överlevnad hos patienterna. Intuitivt vill man såklart genast reducera mängden strålning som levereras till hjärnan. Däremot vet man även att överlevnaden blir sämre om inte tillräckligt hög stråldos levereras till tumören. Inom strålterapi behandlar man alltid med marginaler som ska ta hänsyn till osäkerheter hos tumörens aktuella position och utbredning. Forskare har nu föreslagit en minskning av dessa marginaler. Således skulle detta innebära att en mindre volym frisk hjärnvävnad mottager den höga stråldos som är ämnad för tumören.

I detta examensarbete utfördes en simuleringsstudie med riktiga patientdata, där behandlingsmarginalerna reducerades från 2 cm (nuvarande standard) till 1 cm. Information om recidivens lägen fanns inkluderade för samtliga patienter. Genom att genomföra denna minskning reducerades behandlingsvolymerna med ungefär 40 procent. Intressant nog lyckades stråldosen till frisk omkringliggande hjärnvävnad sänkas utan att behöva offra dos till tumör- och recidivområdena. Man fann även ett samband mellan reducerad behandlingsvolym och reducerad medelstråldos till omkringliggande hjärnvävnad.
Resultaten pekar mot ett potentiellt nytt protokoll för strålbehandling av glioblastom. Säkerställning av dessa resultat samt ifall recidivlägena skulle komma att förändras av att man ändrar på marginalerna återstår att se från framtida kliniska prövningar.

Abstract

Purpose: Improvements in mortality rate of glioblastoma patients have been limited during the past decades, due to the tumor's rapidly growing and infiltrative behavior and resistance to current therapy. Recent findings show that higher brain mean dose strongly correlates with inferior overall survival and that local recurrences mainly occur centrally in previously irradiated regions. This project investigates the possibility of a new radiotherapy protocol for glioblastoma patients, where treatment margins are reduced in order to reduce brain dose while still cover the volume most prone to relapse.

Method: Treatment plans from 45 patients who had been previously treated for glioblastoma, with a prescribed dose of 60 Gy/30 fractions, were used. Recurrence volumes (RV's) were present for all patients. New treatment plans were produced, but with 1 cm clinical target volume (CTV) margins instead of 2 cm (current standard). Additional plans were created for 20 patients, for which a simultaneous integrated boost (SIB) of 75 Gy/30 fractions to the tumor volume was added to the reduced margins tratment plans. The boost volume was defined as a 2 mm margin to a union of the gross tumor volumes (GTVs) from MRI- and PET-scans. The 1 cm CTV was kept with the previous ordinated dose of 60 Gy.
Comparison of doses to target volumes, RV's and OAR's were performed using the Wilcoxon signed rank test in combination with identity plots. Spearman's rank correlation coefficient was used to find whether there is a correlation between the reduction in PTV volume and reduction of brain mean dose as well as dose coverage of RV's and GTV.

Results: A statistically significant reduction in doses was found for whole brain (p<0.001), left eye (p=0.003), right hippocampus (p=0.03) and remaining OAR's (p<0.001). No difference was found for RV's (p=0.30) and PTV (p=0.22). Increased dose coverage was found for GTV (p=0.03) due to some outliers. A statistically significant correlation was found between reduction in brain mean dose and reduction in PTV volume (ρ=0.4, p=0.006).
Evaluating treatment plans with SIB, no significant difference in doses were found for the eyes and hippocampi. The remaining OAR's experienced statistically significant dose reductions (right optic nerve at p=0.005, the rest at p<0.001), while the target volumes and RV's received increased dose coverages (p<0.001).

Conclusion: Reducing the CTV margin from 2 cm to 1 cm may lead to better sparing of OAR's without sacrificing dose coverage of target and RV's. However, clinical trials would need to show whether this would change the recurrence patterns. These will be necessary to find whether the increased local dose coverage following a SIB would actually result in improved tumor control, since we have shown that OAR sparing was not sacrificed. Nonetheless, reducing the irradiated volume without increased treatment side effects would still be of benefit for the patient.

Contents

ABBREVIATIONS

AAA = Anisotropic Analytical Algorithm

CT = Computed Tomography

CTV = Clinical Target Volume

DVH = Dose-Volume Histogram

FLAIR = Fluid-Attenuated Inversion Recovery

GBM = Glioblastoma Multiforme

GTV = Gross Tumor Volume

IMRT = Intensity-Modulated Radiotherapy

MG = Malignant Glioma

MLC = Multileaf Collimator

MRI = Magnetic Resonance Imaging

OAR = Organ At Risk

OS = Overall Survival

PET = Positron-Emission Tomography

PFS = Progression Free Survival

PRV = Planning Risk Volume

PTV = Planning Target Volume

RT = Radiotherapy

SIB = Simultaneous Integrated Boost

TPS = Treatment Planning System

VMAT = Volumetric Modulated Arc Therapy

Chapter 1

INTRODUCTION

There are a variety of different cancer types. Some are more common than others while some are more aggressive. Some are easily surgically removed while others require a combination of different treatment modalities [1]. Glioblastoma multiforme (GBM) is an aggressive form of brain cancer known for its very poor prognosis. Standard treatment consist of surgery followed by combined radiotherapy (RT) and chemotherapy. Despite the complicated treatment plan, local recurrences will be present in the majority of patients [2]. A slight increase in the number of cases have been reported over the past decades, most likely due to diagnostic advancements and people growing older [4, 3]. Therapeutic advancements are of interest, although GBM have proven to be very resistant to current therapy. There has not yet been shown that dose escalation or different fractionation schemes result in better treatment outcome [5]. Some studies have shown that the vast majority of recurrent tumor volumes (RV) are located within the treatment volume [5, 6]. It has been shown that a higher mean dose to the whole brain is associated with inferior progression free survival (PFS) and overall survival (OS) [7]. Therefore, there is an interest in reducing the treatment margins, and thus the mean brain dose, and see if this will result in any changes regarding the recurrence patterns.

1.1 Aims

The overall goal with this project was to investigate whether it would be reasonable to carry out a clinical study regarding reducing the treatment margins for glioblastoma patients. As a side project, dose escalation plans were made for half of the margin reduced treatment plans. The data obtained were used in order to answer the following questions.

1. Can we reduce the clinical target volume margins from 2 cm to 1 cm while still maintaining acceptable dose coverage of the recurrence volumes?
2. Is there a correlation between target treatment volume and brain mean dose?
3. Is a simultaneous integrated boost (SIB) for the margin reduced plans viable from

a perspective of recurrence volume coverage, mean brain dose and organs at risk sparing?

Chapter 2

THEORETICAL BACKGROUND

2.1 Glioblastoma

Our cells are constantly being renewed through cell division. Cells that become old or damaged undergo apoptosis, also known as programmed cell death [8, 9]. If this process is hindered, abnormal cells may proliferate uncontrollably and form solid tissue masses called tumors. If these have the capacity to grow and spread into surrounding tissues, they are called malignant tumors. Although surgically removed, malignant tumors may recur if there are cancer cells still present at the resection area [9].

Brain tumors belong to the less common types of cancers. Malignant gliomas are diagnosed in about 6 out of 100 000 people worldwide. Among these, GBM is both the most common and the most aggressive form that originates from within the brain [2, 10] (figure 2.1). World Health Organization (WHO) grade tumors of the central nervous system based on several pathological characteristics, ranging from grade I to IV. Grade I tumors are defined by their slow growth and are considered nonmalignant, while grade IV display rapid growth and are very malignant. GBM is cathegorized as grade IV [11]. With treatment the median overall survival is around 15 months while the same figure for non-treated patients is around 3 months [10, 12]. One main reason behind its poor prognosis is its ability to spread, via white matter tracts, throughout the brain before manifesting any symptoms [16, 13]. These symptoms may include headaches, seizures, and hemiparesis among others, depending on the tumor site [13].

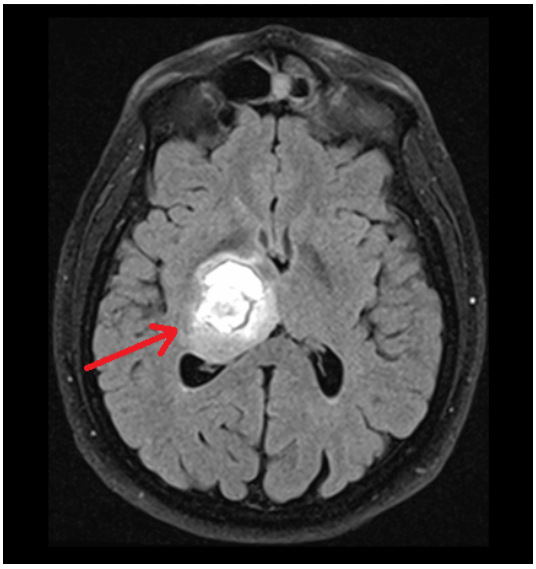

Figure 2.1: Patient with GBM from this cohort as shown on an MRI T2/FLAIR scan. The tumour is shown as a bright area in the right hemisphere. Deformation of the right lateral ventricle is clearly visible (red arrow).

2.1.1 Neoplasm post-radiotherapy

The definition of post-radiotherapy tumour progression for glioblastoma has been a topic of discussion throughout the years. Difficulty in, for instance, assessing whether the contrast-enhanced components really represent true progression (i.e. high risk of pseudoprogression) led to Wen et al. proposing an updated response criteria in 2010 (the RANO response criteria) [14]. The criteria include how to assess new lesions, enlargement of enhancing as well as nonenhancing lesions, taking into account of corticosteroid doses and various treatment effects. Implementation of additional T2/FLAIR imaging for measurement of nonenhancing lesions is a big difference to the old MacDonald response criteria, which only took into account T1-weighted gadolinium enhanced lesions (and computed tomography (CT) lesions) [14, 15].

2.1.2 Current therapy: summary

As of today, standard treatment consist of maximum safe surgical resection of the tumor followed by external RT to the resection area [2, 10]. Radiation is given concurrent with temozolomide, a chemotherapy drug also functioning as a radiosensitizer. RT is delivered over the course of six weeks as 60 Gy divided over 30 fractions [2]. Patients with a worse survival expectancy are given higher doses per fraction over a shorter time period. Studies have not been able to show that either radiosurgery, brachytherapy or exceeding 60 Gy for external RT result in improved survival [5]. With the emerged knowledge about glioma stem cells and their resistance toward standard radiation and chemotherapy, some researchers believe that emphasis should be laid on the development of targeted drug, chemo- and immunotherapy [12].

2.2 Radiotherapy

In radiotherapy, ionizing radiation is used in order to inflict damage to the DNA in cells. Cancer cells are less prone to DNA reparation compared with normal tissue cells. This is the main principle behind fractionated RT, where small radiation doses are given normally one day apart in order for normal tissue to recover in between fractions. This enables tumor control while minimizing normal tissue damage, i.e. possible treatment side effects. Radiation absorbed dose is measured as the amount of energy deposited in tissue mass and is commonly denoted as Gray (1 Gy = 1 J/kg). Radiation can be used in both curative and palliative treatments of most cancers [8, 17, 18].

There are several methods of radiotherapy, including: radioisotope, brachy- and external beam radiotherapy. The former utilizes a radioisotope that is normally orally or intravenously distributed to the patient. Brachyterapy utilizes sealed radioactive sources that are placed into the tumor tissue. These sources can either be permanent or removable, depending on the treatment. External beam RT uses a gantry that shapes

and focuses a radiation beam onto the desired treatment area [8, 17].

2.2.1 External beam radiotherapy

The external RT beam can consist of photons, electrons or heavier charged particles [8, 17, 18]. These beams can be produced in different ways. For example, a photon beam can either be produced by a linear accelerator or a radioactive cobalt-60 source. What ever radiation type is used, the concept is to manipulate the intensity (only linear accelerator) and shape of the beam, using various filters and collimators in the gantry head, to fit the treatment area. Most often, radiation is delivered to the tumor at various different angles around the patient. Distributing the radiation dose to normal tissue over a larger volume lowers the risk for deterministic effects of radiation dose. Today's external RT machines are equipped with on board imaging techniques to assist the staff in delivering more accurate and precise treatments [17, 18]. A simplified illustration of a RT machine without on board imaging is shown in figure 2.2.

Figure 2.2: Radiotherapy machine with a rotating gantry, enabling treatment at different angles. Some treatment tables are able to rotate in order to enable more incidence angles.
Image taken from:
http://www.prostatecancercentre.ca/ pcc-faqs/external-beam-radiation/

2.2.2 IMRT and VMAT

Modern external RT machines have a setup of different collimators in the gantry head in order to shape the radiation beam. The newest addition of these are the multi-leaf collimators (MLC), consisting of a large number of high atomic number material "leaves" that can move individually to shape the beam [17]. The implementation of MLCs has enabled two of the most frequently used treatment techniques: intensity modulated radiation therapy (IMRT) and volumetric modulated arc therapy (VMAT).

IMRT and VMAT enables intentional inhomogeneous dose distribution, using so called ”inverse treatment planning” which will be touched upon more in section 2.2.5. This means a more conform target coverage, enabling dose escalation, and more normal tissue sparing, reducing risk for late radiation toxicity. These two factors are especially valuable when having complex shaped target volumes located near vital organs. This treatment delivery technique builds upon being able to control the intensity and shape of the beam at each gantry angle, using the MLC. One common method is, for each

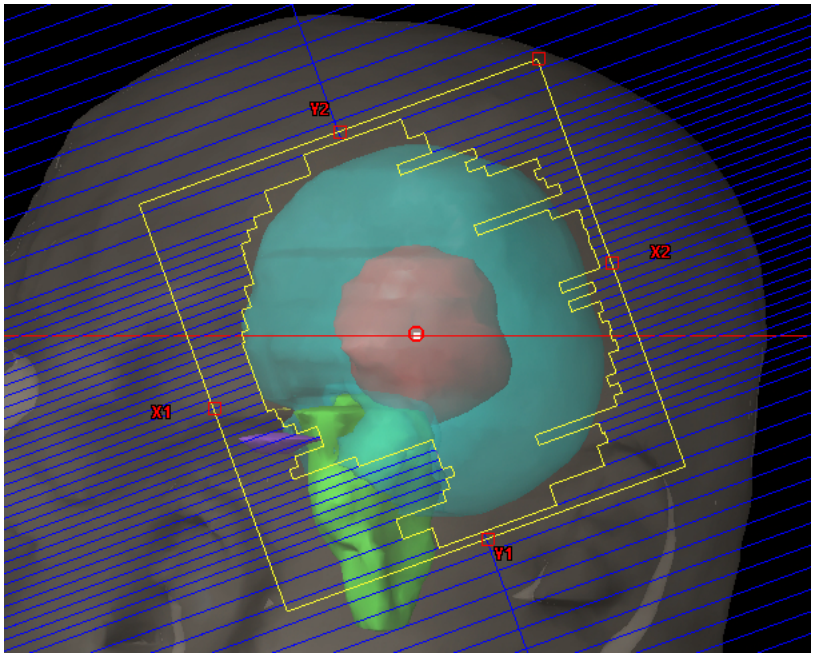

Figure 2.3: A beam's eye view from one of the fields of a VMAT treatment plan as shown in Eclipse™. The MLC is shown as blue lines. The inner yellow structure represents the aperture at a specific gantry angle while the outer yellow structure represents the maximum open field, defined by the jaws of the accelerator, for this treatment plan. Also shown in the image are the GTV (red), PTV (blue), brainstem (green) and hippocampus (purple) structures.

preset gantry angle, to have a set of differently shaped fields contributing to an inhomogeneous dose distribution. The sum of the fields from all gantry angles then contribute to a homogeneous dose distribution across the treatment area. Another commonly used method for reaching this homogeneity is to have the MLC moving continuously while delivering radiation at each treatment angle [19].

VMAT can be seen as a further development of IMRT. Instead of having specific preset treatment beam angles, VMAT involves a continuously rotating gantry during treatment delivery. Thus, having the MLC moving simultaneously enables shorter treatment delivery time [20]. A beam's eye view of a field from a VMAT treatment plan in Eclipse™ Treatment Planning System (TPS) (v. 13.6, Varian medical systems, Palo Alto, CA, USA) can be seen in figure 2.3.

2.2.3 Simultaneous integrated boost (SIB)

Local recurrences post radiotherapy are a present concern. A need for increased tumor control has lead to several methods of escalating the radiation dose to the treatment areas, or shorten the total treatment time by increasing the fraction dose. One of these methods, commonly used in the past, is the IMRT sequential boost. The principle is to deliver a sequential radiation field, or fields, thus delivering different total doses to different regions of the target. The technique currently in use is called a simultaneous integrated boost (SIB). The SIB-IMRT delivers different doses to different regions of the target volume in one session, thus making it a more conformal and effective treatment. By increasing the dose only to the tumor bed inside of the target volume, increased tumor control may be achieved without sacrificing neighboring normal tissue [21].

2.2.4 Target volumes & treatment margins

When creating a treatment plan, certain structures such as organs and tumours need to be defined and delineated. The delineation may be done either manually or automatically. The volume structure representing the tumour, as demonstrable from diagnostics, is called the GTV (red delineated structures in figure 3.1). The GTV usually contains the areas with the highest tumour cell density. In cases were the tumour has been removed, there may not be a GTV present. The clinical target volume (CTV) serves as an outer margin and contains the GTV (pink delineated structure in figure 3.1). The CTV represents the uncertainty in GTV delineation since there may be microscopic spread outside the "visible" GTV [22]. In cases when there is no GTV, the CTV is drawn from the original tumour site [23]. Geometric uncertainties are taken into account for with the planning target volume (PTV), which is an additional outer margin to the CTV (blue delineated structures in figure 3.1). These geometrical uncertainties include variation in patient positioning between treatments and internal tumour movement as well as uncertainties in treatment delivery. All non-target tissues that are taken into account in treatment planning are called organs at risk (OAR). Examples are brainstem, chiasma and optic nerves (shown as green, and yellow structures in figure 4.5). Radiation doses to the OAR are to be kept as low as possible while still delivering a sufficient amount of radiation to the target volumes. As with the CTV, OAR also come with geometrical uncertainties. Thus, a planning risk volume (PRV) may be added, functioning as an additional safety margin of the OARs. These are of particular importance for serial organs like the brainstem, where high radiation doses to a small volume of the organ can have a considerable impact on the organ's function. [22, 23, 24].

In the case of radiotherapy of glioblastoma patients the CTV margins are usually around 2-3 cm from the GTV, however there are no universal guidelines regarding these. This is due to the highly diffuse microscopic spread of the tumour, making the choice of a CTV margin rather complicated. The question is therefore not how large margins are required to contain the tumour cells, but rather what proportion of the tumour is considered sufficient to treat [25, 26].

2.2.5 Treatment planning

When creating a VMAT treatment plan, inverse planning is used. Forward planning involves the treatment planner determining the number of fields and how these are to be positioned and shaped. Reversed planning utilizes an iterative optimization program to obtain a suitable treatment plan. The optimizer works from certain dose constraints set by the planner. These include maximum, minimum and mean doses to specified target and organ at risk (OAR) volumes, as well as doses received by parts of these volume ($D_{2\%}$, $D_{50\%}$, $D_{95\%}$ etc.). Along with these, relative values of priority are given to each constraint. When all is set, the software optimizes MLC shape, dose rate and gantry rotation speed for each angle of the arc in a number very simplified steps. Firstly, a couple of fixed angles are chosen for optimization. These couple of "static"

fields basically divide the arc into smaller arcs. Secondly, these smaller arcs are once again divided into even smaller ones which are optimized. The process continues until the optimizer has gone through a certain number of so called multiresolution levels [20].

2.2.6 Dose-volume histogram

The dose-volume histogram (DVH) is the most central tool for evaluating treatment plans. The basic principle is that each voxel in the irradiated volume is sorted into a dose bin. Each dose bin is defined by a dose interval, containing only voxels receiving doses within these intervals. Plotting the number of voxels in each bin against their respective dose intervals gives us a *differential DVH*. However, if one would instead define each bin by a minimum dose, then we would have a *cumulative DVH*. Normally, a cumulative DVH plots the volume of a structure that receives a certain dose or higher against this certain dose [27]. Since the voxel size is known, the number of voxels in each bin is easily converted into a volume. The cumulative DVH is the one used clinically when evaluating and comparing treatment plans (see figure 2.4).

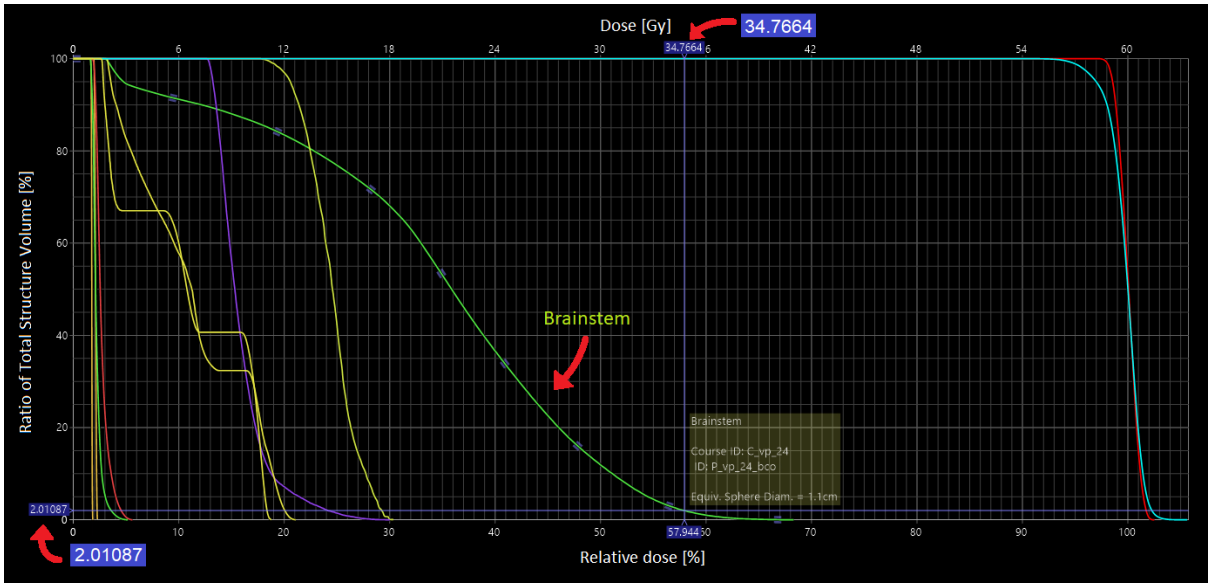

Figure 2.4: A cumulative dose volume histogram showing ratio of total structure volume versus dose. The different structures are represented by the differently colored graphs. For example, one can see that 2% of the brainstem, represented by the green graph, receives at least 34.8 Gy.

The DVH is used when verifying whether a treatment plan meets the dose constraints or not. DVH-data such as maximum, minimum and mean doses, as well as what doses a certain structure volume size receives, are readily available. In figure 2.4, the lowest dose (34.8 Gy) received by 2% of the brainstem structure volume is highlighted. There is on the other hand no spacial information of the dose distributions, meaning that the DVH is only a complementary evaluation tool. For example, when comparing the DVHs for a certain OAR between two treatment plans, one could easily see if one of

the structures completely receives lower doses compared with the other. However, if the DVHs for the two structures would cross around midrange, then only using DVH data would be insufficient since we might just have a redistribution of the doses [27].

2.3 Imaging modalities: CT, MRI & PET

CT is a medical imaging technique where x-ray is used in order to generate three dimensional anatomical images. This method utilizes the principle that x-ray is absorbed to varying extends depending on tissue density. Therefore, CT images are basically anatomical density maps [28]. These are frequently used in radiotherapy treatment planning [29]. The brain scans on the middle and bottom rows in figure 3.1 are CT scans.
Positron emission tomography (PET) also uses radiation in order to create anatomical images. However, PET uses radiopharmaceuticals that are intravenously injected in the patient. Uptake of the pharmaceuticals are normally increased for lesions and tumors. By detecting the photons from the radionuclide, the tumor or lesion locations can be determined, making PET invaluable for detecting tumors [30, 31]. Since PET-images suffer from poor spatial resolution, they are normally combined with CT-images in order to get better localization of the uptake region [31]. The top left brain scan in figure 3.1 is a PET/MRI scan.
Apart from the previously mentioned imaging modalities, magnetic resonance imaging (MRI) do not involve ionizing radiation. Instead, magnetic fields and radio waves are used in order to acquire radiofrequency signals from protons of the patient. These signals are then used to create the anatomical images [32]. The superior detail in imaging of soft tissues makes MRI the current standard for defining tumors in the brain [33]. The left and middle brain scans of the top row in figure 3.1 are MRI scans.

Chapter 3

MATERIALS AND METHODS

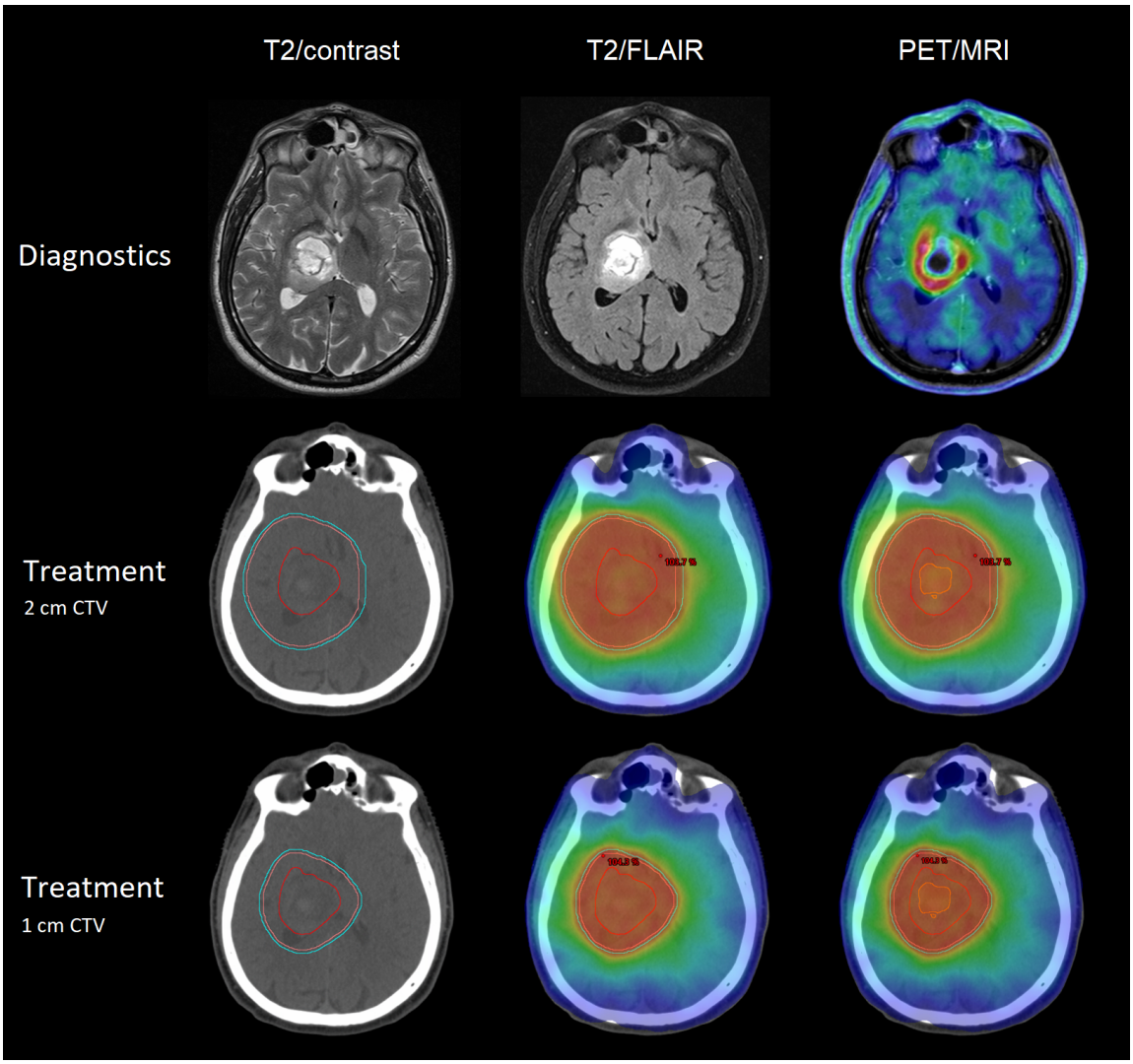

Figure 3.1: Top row: Images of a brain with glioblastoma obtained using MRI/T2 with contrast (left), MRI/T2 FLAIR (middle) and PET/CT (right). Middle row: Treatment planning CT showing GTV (red), standard 2 cm CTV (pink) and PTV (blue). A simulated dose distribution of the finished treatment plan is shown in the second image and an additional RV (orange) is included in the third image. Botton row: Same as the middle row but with the new 1 cm CTV instead.

3.1 Treatment planning

Treatment plans from 45 patients, who all underwent imaging and treatment at Rigshospitalet in Copenhagen, Denmark, in 2011-2013 were used for this project. Their prescribed treatment dose were 2 Gy x 30 fractions. All patients had recurrences and underwent additional PET/MRI after radiotherapy. RV's where available for all patient structure sets. Current dose planning constraints at Rigshospitalet were used during replanning (table 3.1). All treatment plans were created in Eclipse™ TPS. The original plans were calculated using an Anisotropic Analytical Algorithm (AAA) with 2.5 mm grid size while the new plans used Acuros-XB® with 1 mm grid size, since this is the current standard in the clinic. The two algorithms, according to litterature, give very similar calculated doses [34]. Ten of the new plans were recalculated using AAA and 1 mm calculation grid size in order to verify any potential deviations between both the calculation algorithms and different grid size.

Table 3.1: Current dose constraints for treatment planning of brain tumours with 60 Gy/30 fractions at Rigshospitalet in Copenhagen, Denmark.

2 Gy x 30 fractions	
Structure	*Constraint*
Brainstem	-
Brainstem_Inner	54 Gy
BrainstemSurface	60 Gy
Brainstem_PRV	60 Gy
SpinalCord	45 Gy
SpinalCord_PRV	50 Gy
Brain-GTV	$V_{30} < 50$ %
Chiasm	54 Gy
Chiasm_PRV	60 Gy
OpticNerves	54 Gy
OpticNerves_PRV	60 Gy
EyeFront	30 Gy
EyeBack	45 Gy
Lacrimal	$D_{mean} \leq 25$ Gy
Cochlea	$D_{mean} \leq 45$ Gy $D_{5\%} \leq 55$ Gy
Parotid	$D_{mean} \leq 26$ Gy
Lens	5 Gy
Pituitary	$D_{mean} \leq 20$ Gy $D_{40\%} \leq 7.3$ Gy
Hippocampus	$D_{mean} \leq 10$ Gy $D_{max} \leq 16$ Gy

3.1.1 Reducing CTV margins

Replanning the original treatment plans basically included copying these, modifying the structure sets and optimizing/-calculating the new plans. The GTV used for planning consisted of the GTVs delineated from the PET and MR images. The new CTV structure was created as a 1 cm outer margin to the GTV and then cropped to the old CTV. The old CTVs had often been manually modified to avoid certain structures and would therefore at times fall below 1 cm. A new 2 mm PTV margin was added to the new CTV (botton row figure 3.1.

3.1.2 Additional structures for OARs

PRV's were added to brainstem, chiasma and the optic nerves as 1 mm outer margins. Two additional structures, BrainstemSurface (3 mm wall of Brainstem) and Brainstem_Inner (the difference between Brainstem and BrainstemSurface), were added since these are included in the current dose constraints. OARs of interest were brainstem, chiasma, optic nerves, eye, lens, hippocampus and Brain-GTV (the whole brain excluding the GTV). In cases with any of these missing, they were added to both the old and new plans. When added to the old plans, these were not reoptimized for the new structure. Eyes (divided into front and back), lacrimal gland, cochlea, parotid and pituitary glands were excluded in the new plans since none of the old plans included them. However, Eye was included in both plans and thus was taken into account when making the new plans.

The new treatment plans were reviewed and deemed clinically acceptable by a senior medical physicist and a radiologist, as well as a radiation oncologist.

3.1.3 Dose-escalation through SIB

Twenty of the patient plans having had reduced CTV and PTV margins were randomly selected for additional modification. A new inner PTV was created as a 2 mm outer margin from a union of GTV_{MRI} and GTV_{PET} with a prescribed dose of 75 Gy [35]. The previous PTV (1 cm CTV + 2 mm) was kept with the 60 Gy prescribed target dose as before.

3.2 Data analysis

The treatment plan data in DICOM-format (structure-set, dose matrix and plan information) were exported manually from Eclipse™. DVH-data for each structure were obtained from the DICOM-files using MATLAB, release 2014b (The MathWorks, Inc., Natick, MA, USA). $D_{2\%}$ were obtained for brainstem, chiasm, optic nerves, eyes and lenses, $D_{40\%}$ for hippocampi, D_{mean} for brain and $D_{95\%}$ for GTV and PTV. $D_{2\%}$ was used instead of D_{max} since the maximum dose might correspond to a negligible volume, e.g. a voxel. Identity plots were created for all structures in order to get a direct comparison between the plans (see Appendix A). A scatter plot with a linear regression showing differences in mean brain dose versus differences in PTV volumes was also created, as well as a histogram of the percentage reduction in PTV volumes.

3.3 Statistical analysis

MATLAB was used for all statistical analysis. Since the data samples are paired (same patient) and we do not assume that the DVH-data follow a normal distribution, thus the Wilcoxon signed-rank test was used for comparing doses to the OARs of interest as well as the PTVs, GTVs and recurrence volumes [36]. For the same reason, Spearman's rank correlation coefficient was used to investigate the potential correlation between the brain mean dose and PTV volume [37]. The same analysis was performed between GTV dose coverage and PTV volume, as well as RV dose coverage and PTV volume analysis. All values of $p<0.05$ were considered statistically significant.

We wanted to estimate to what extend the overall survival from Munck af Rosenschöld et al. [7] would be affected by our results (the difference in mean brain dose). Unfortunately, this was considered too uncertain since they had used a multivariate Cox Model with internally dependent variables.

Chapter 4

RESULTS

4.1 Reducing CTV margins

4.1.1 Mean brain dose & recurrence volume coverage

One patient was excluded due to the old CTV margin being only 1.5 cm. The left and middle plots in figure 4.1 show how the mean dose to the brain as well as the RV dose coverage differs between the original and the new treatment plans. All doses are presented as absolute doses, in Gray.

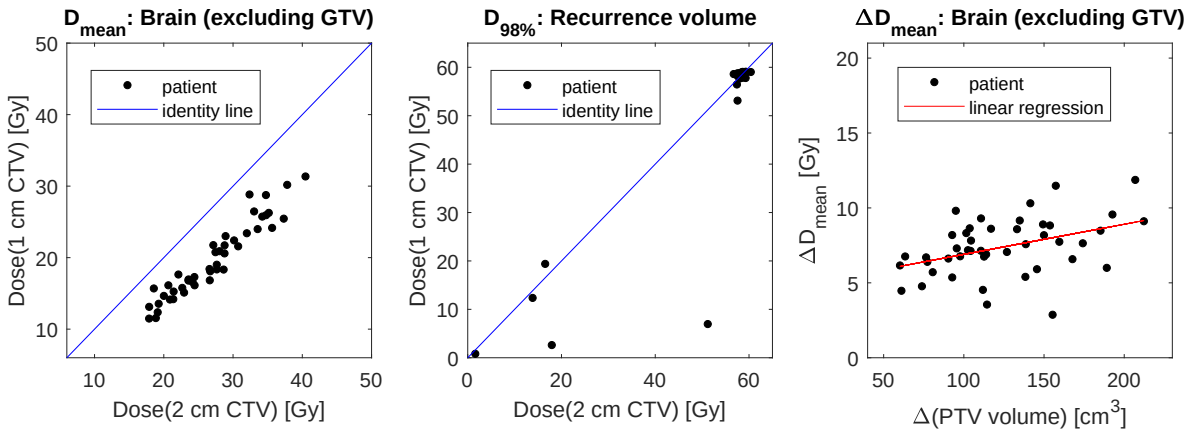

Figure 4.1: Identity plots for brain mean dose, excluding GTV, (left) and RV $D_{98\%}$ (middle). Difference in brain mean dose between the original and new treatment plans plotted against their differences in PTV-volume (right). The linear regression shows a moderate positive correlation with a coefficient ρ=0.4 (p=0.006).

The brain mean dose is consistently and significantly lower for the new treatment plan. Concerning RV dose coverage, no statistically significant difference (p=0.31) comparing the two treatment plans was found. Most recurrences were located inside the PTV defined on the pre-treatment imaging.

The right plot in figure 4.1 shows a statistically significant correlation (p=0.006) between the reduction in brain mean dose and the reduction in PTV volumes. The GTV and RV coverages were not statistically significantly correlated to the reduction in PTV volume (see table 4.1). The histogram in figure 4.3 shows that most patients experience a PTV volume reduction of around 40 percent from reducing the CTV margins to 1 cm.

Table 4.1: Upper section: Spearman's rank correlation test results for investigating correlations of brain mean dose, GTV and RV with differences in PTV volumes. Lower section: Wilcoxon signed rank test results for comparing doses to OAR structures of interest, target structures and RV's of the 2 cm and 1 cm CTV treatment plans. Bold values implies p <0.05.

Spearman's Rank Correlation

Δ(PTV volume) vs.	n	ρ	p
	45		
ΔD_{mean}: Brain (excluding GTV)		0.40	**0.006**
$\Delta D_{98\%}$: Recurrence volume		-0.16	0.29
$\Delta D_{95\%}$: GTV		-0.079	0.61

Wilcoxon Signed Rank Test

Structure	n	p
	45	
$D_{2\%}$: Brainstem		<**0.001**
$D_{2\%}$: Chiasm		<**0.001**
$D_{2\%}$: Optic Nerve (Left)		<**0.001**
$D_{2\%}$: Optic Nerve (Right)		<**0.001**
$D_{95\%}$: GTV		**0.03**
$D_{95\%}$: PTV		0.22
$D_{98\%}$: Recurrence volume		0.31
$D_{2\%}$: Eye (Left)		**0.003**
$D_{2\%}$: Eye (Right)		<**0.001**
$D_{2\%}$: Lens (Left)		<**0.001**
$D_{2\%}$: Lens (Right)		<**0.001**
$D_{40\%}$: Hippocampus (Left)		<**0.001**
$D_{40\%}$: Hippocampus (Right)		**0.03**
D_{mean}: Brain (excluding GTV)		<**0.001**

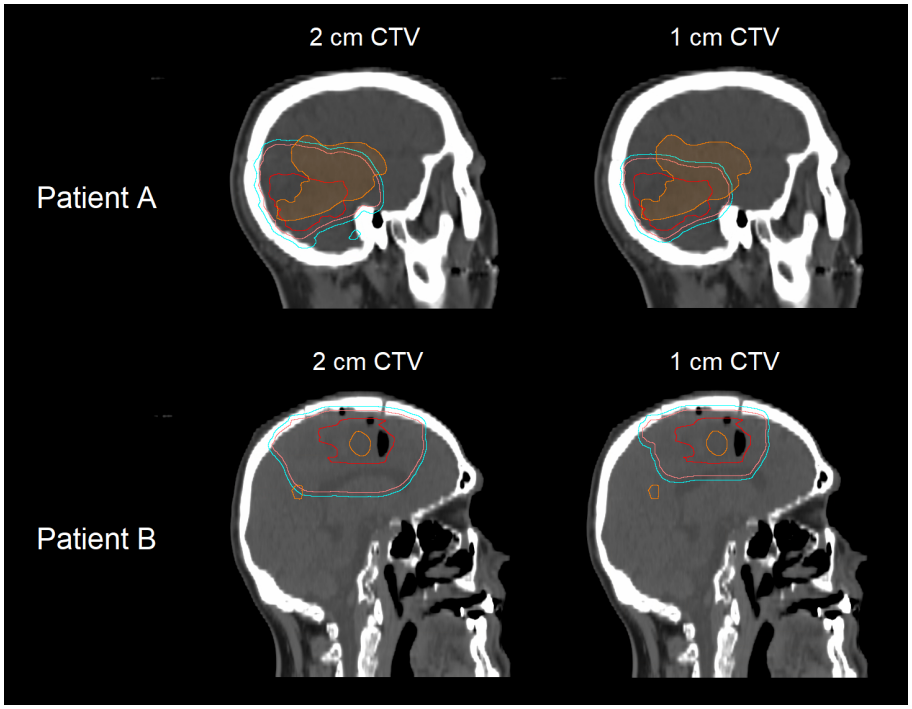

Figure 4.2: Sagital CT images with contours superimposed for two patients where the RV coverages were drastically impaired after decreasing the treatment volumes. The delineated RV in Patient A was very large while Patient B showed multifocal recurrence, with only one of them contained by the old PTV. The RV is represented by the orange structure.

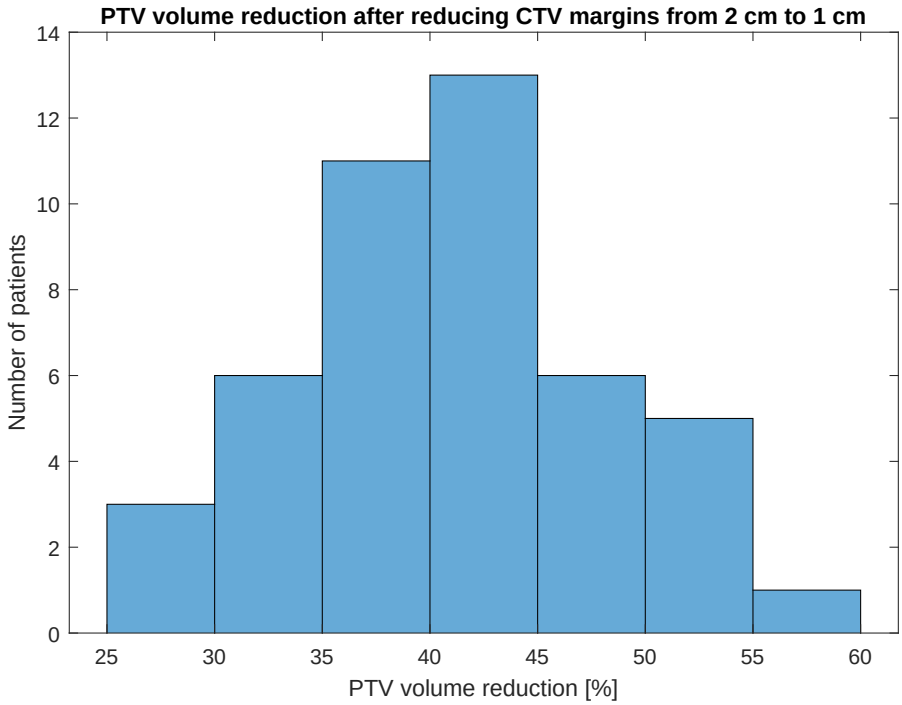

Figure 4.3: Histogram showing the percentage PTV volume reduction of the 45 patients due to shrinking the CTV margins from 2 cm to 1 cm.

4.1.2 Organs at risk

All OAR's showed a trend towards a statistically significantly lower dose when using the reduced CTV margins. Comparing GTV coverages ($D_{95\%}$) yielded statistical significance (table 4.1), however this difference indicates an improvement which is evident by studying the identity plot for $D_{95\%} : GTV$ in appendix A.1. The treatment plan corresponding to the data point located second furthest to the left is presented in figure 4.4. Due to the reduced CTV margin, the new plan could achieve a better GTV coverage and lower doses to the brainstem and chiasm. For this patient, the new plan also resulted in higher doses to both eyes, left optic nerve and left hippocampus, although all were within the constraints.

Tumour sites located very close to or even adjoining OARs were fairly common in the original treatment plans. These patients in particular would experience a considerable dose reduction to the OARs when implementing 1 cm CTV margins. Figure 4.5 shows one of these patient situations, having the GTV going into the brainstem. Here we try to keep the brainstem dose the same as the old treatment plan, however doses to the chiasm and optic nerves could be considerably reduced by more than 20 Gy to each. GTV coverage was also improved with the new CTV in this situation.

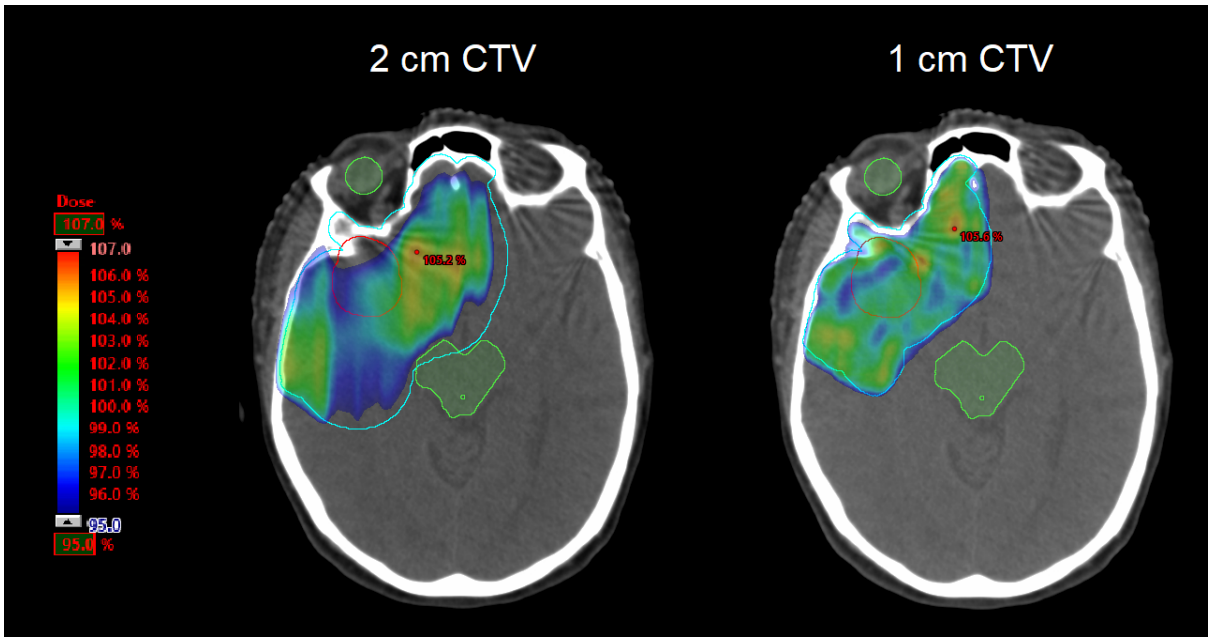

Figure 4.4: Left: Old treatment plan with inferior GTV coverage. Right: New patient plan with improved GTV coverage but higher doses to the eyes and the left optic nerve. This is an example of when one needs to consider whether to prioritize target coverage over OAR's and vice versa. 100% dose corresponds to the prescribed target dose, 60 Gy.

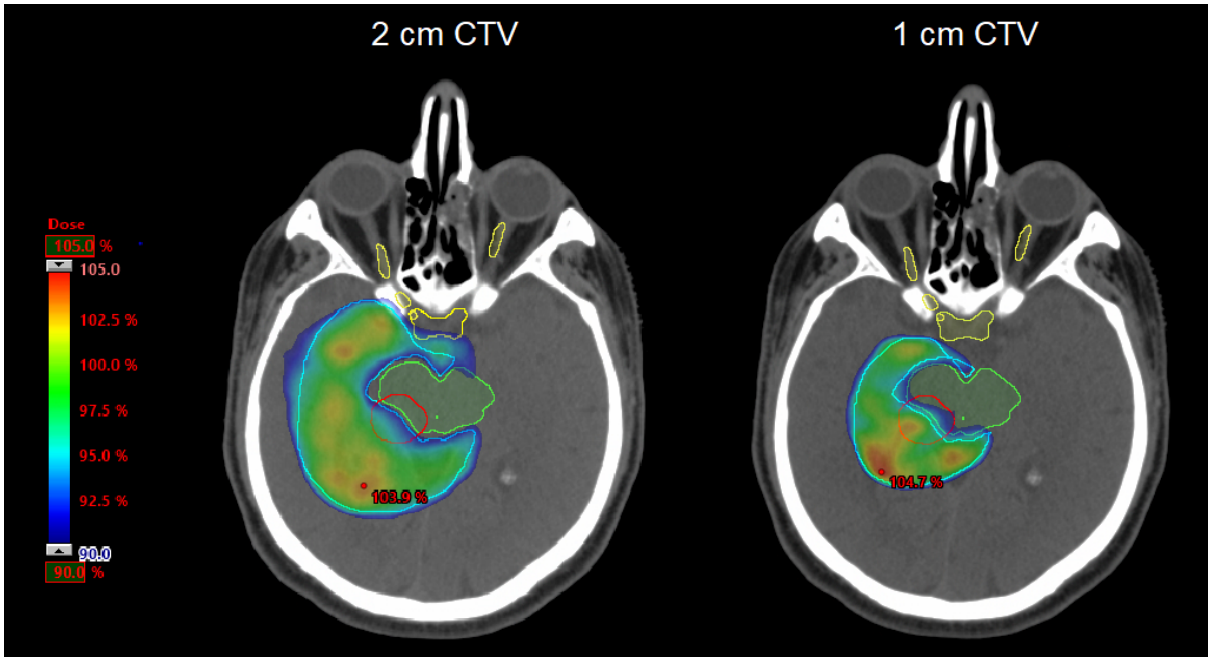

Figure 4.5: Patient with the tumour partially located inside the brainstem. The PTV was cropped for dose sparing of the brainstem, chiasm and optic nerves. 100% dose corresponds to the prescribed target dose, 60 Gy.

4.2 Acuros-XB vs. AAA

The identity plots in appendix A.3 show little variation compared to the identity plots in appendix A.1. To summarize, the largest deviations for these are 0.53 Gy (PTV), 0.31 Gy (GTV), 0.26 Gy (Lens L), 0.33 Gy (Lens R), 0.64 Gy (Eye L) and 0.96 Gy (Eye R).

4.3 Reducing CTV margins in combination with SIB

4.3.1 Mean brain dose & recurrence volume coverage

Figure 4.6 presents identity plots of the brain mean doses (left) and RV D_{98} doses (right) respectively for the 20 patients involved. Wilcoxon signed rank test results are presented in table 4.2. It is clear that the brain mean doses were still significantly lower after adding the SIB. However these doses were slightly higher than for the reduced margins only treatment plans. The RV doses were significantly higher, although fairly evenly distributed between 58 and 74 Gy, with half of the doses lying between 70 and 74 Gy.

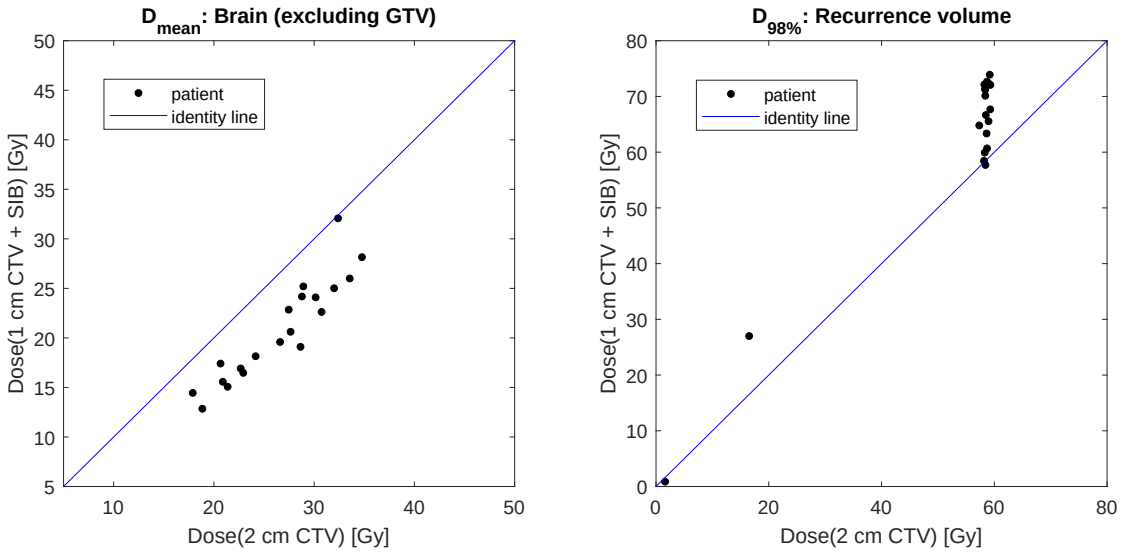

Figure 4.6: Identity plots for brain mean dose, excluding GTV (left) and RV $D_{98\%}$ (right).

Table 4.2: Wilcoxon signed rank test results for OAR structures of interest, target structures and RV, comparing the old treatment plans (2 cm CTV) and new modified treatment plans (1 cm CTV including SIB). Bold values implies $p < 0.05$.

Wilcoxon Signed Rank Test		
Structure	n	p
	20	
$D_{2\%}$: Brainstem		<**0.001**
$D_{2\%}$: Chiasm		<**0.001**
$D_{2\%}$: Optic Nerve (Left)		<**0.001**
$D_{2\%}$: Optic Nerve (Right)		**0.005**
$D_{95\%}$: GTV		<**0.001**
$D_{95\%}$: PTV		<**0.001**
$D_{98\%}$: Recurrence volume		<**0.001**
$D_{2\%}$: Eye (Left)		0.77
$D_{2\%}$: Eye (Right)		0.87
$D_{2\%}$: Lens (Left)		**0.001**
$D_{2\%}$: Lens (Right)		<**0.001**
$D_{40\%}$: Hippocampus (Left)		0.09
$D_{40\%}$: Hippocampus (Right)		0.06
D_{mean}: Brain (excluding GTV)		<**0.001**

4.3.2 Organs at risk

Identity plots for the OARS are presented in appendix A.2. These plots together with table 4.2 show that only the eye and hippocampus doses were not significantly reduced for the SIB plans. In appendix A.2, one can see that as the eye dose increases for the old treatment plans, these doses get worse for the SIB-plans. For the left hippocampus, higher doses for the SIB-plans tend to correspond to old treatment plans with hippocampus doses around 60 Gy, the ordinated target dose. There seems to be no particular trends for doses to the right hippocampus.

Chapter 5

DISCUSSION

The large reduction in PTV volume would mean that a lot of normal tissue could be spared. The benefit of decreasing the treatment margins may be location dependent since tumours with a CTV that is already cropped to any extent (e.g. to the skull) will experience a smaller relative volume reduction compared to tumours with uniform CTV margins.

The mean brain dose trend as well as the stable RV dose coverage turned out as expected when decreasing the treatment margins. Out of the 45 patients, two deviant data points are present in the middle plot of figure 4.1. One patient had an unusually large RV with parts of it already extending outside the old PTV (patient A in figure 4.2). The other patient had multifocal recurrences with one of the tumors located partially outside the old PTV (patient B in figure 4.2). One could argue that since the original margins already do not cover large parts of these volumes, it would not make a big difference. It is still important to consider the risk of impaired tumor control for these patients, since our aim is to at the very least not worsen their already poor life expectancy. Only a clinical trial could prove whether the suggested reduced CTV margins should be implemented into the treatment planning standard, since we do not know how the new CTV would affect the pattern of local recurrences. Nonetheless, this suggestion for a clinical study could further be supported by the results of Munck af Rosenschold et al., showing an association of large mean brain dose and worse PFS and OS [7]. The potential patient benefit would be the possible reduction of the development of radiation necrosis [38]. Before such a clinical trial can be initiated, effort must also be put into managing uncertainties in the treatment delivery. Smaller margins means less room for uncertainties, which may require more frequent imaging or even adaptive radiotherapy.

The doses to OAR's were fairly scattered compared to the more consistent correlation seen for the mean brain dose. Since locations of the OAR's in relation to the target volumes vary largely among the patients, we could expect a large variation in dose differences between the treatment plans as well. For example, as seen in appendix A.1, in cases where the treatment volume was located close to the brainstem, target coverage was prioritized over brainstem dose to a greater extent for the new treatment plans. However, these still fulfilled the constraints of table 3.1. Another clear example are

the hippocampi. Apart from those receiving around 60 Gy, most data points from the plot $D_{40\%}$*: Hippo R* are located at around 5-15 Gy for the new treatment plans, which conforms with the current dose constraints (note that hippocampus is least prioriated in table 3.1). Since it has been suggested that memory preservation and quality of life is associated with hippocampi dose avoidance [39, 40], it could be reasonable to try to meet the dose constraints for at least one of them. This could especially be of importance if the overall survival of glioblastoma patients should rise.
Like with the hippocampi, the eyes also have many data points located above the identity line (plots $D_{2\%}$*: Eye L/R* in appendix A.1). The distribution of data points along this line is likely due to the new constraints allowing higher doses. Though, a statistically significant dose reduction was shown for both eyes and all new treatment plans stayed within the dose constraints of EyeFront and EyeBack there are at least two new alternatives one could go by from these results. Keeping the smaller CTV and try to keep eye doses as low as possible, or allow higher eye doses in favor of target coverage or sparing of other OARs. The latter alternative could possibly make it easier to enable a dose escalation trial, however this one should be approached cautiously.

The two patients in figures 4.4 and 4.5 were the main cause to the GTV comparison being significant. Otherwise the data looks fairly evenly distributed along the identity line. In figure 4.4, one could say that the dose distribution has been moved upwards since the location of the GTV being so close to the bone structure behind the right eye socket. This could be worth noting when modifying the margins to a GTV located close to the skull, where the old CTV is already cropped to a great extent in one direction.

From the identity plots in appendix A.3 It is apparent that AAA give higher calculated doses to the target volumes, left eye and right lens. Although, this difference is small compared to the difference we see when comparing CTV margins and should therefore not affect our results. The study by Kathirvel et al. comparing Acurox-XB and AAA showed that both algorithms had high calculation accuracies but that AAA tended to slightly overestimate the delivered doses.

In comparison with the original treatment plans, the brain mean dose is still kept lower for the SIB-plans (left plot in figure 4.6). Dose coverages of the local recurrences were clearly improved (right plot in figure 4.6). The distribution of the magnitude of improvement varied due to the recurrence structures being in different shapes, sizes and locations, therefore not always being fully contained by the initial GTV structure. Munck af Rosenschold et al. showed that inferior dose coverage of the GTV was associated with inferior OS [7]. If better tumor control could be combined with lower radiation doses to the rest of the brain, this could be a small stepping stone in the development of new therapeutic protocols for glioblastoma patients.
Furthermore, compared to the original treatment plans, radiation doses to most of the OARs were lower for the SIB-plans. The eye doses were higher for eight of the SIB-plans. Their relatively moderate sizes (only brainstem is larger), and harder constraints (excluding lenses), result in eye doses being more difficult to keep low compared to other OAR's. Radiation doses to the lenses, which are part of the eyes, are

nonetheless clearly reduced for the SIB-plans (plots $D_{2\%}$*: Lens L/R* in appendix A.2). The high doses to left hippocampi were due to being located close to or partly inside the target volumes. A dose-escalation to the GTV would not unexpectadely lead to larger doses to hippocampi located near or in the vicinity of the GTV. Neither hippocampi or eye doses were statistically significantly higher for the SIB-plans (table 4.2), however this is very patient specific.
Although it has not been clinically shown that patients treated with a $GTV_{MRI+PET}$ necessarily have better overall or progression free survival [7], it could still be interesting to implement the PET-volumes into the margin reducing trials (regardless of dose escalations).

Chapter 6

CONCLUSION

This study has shown that in theory it is possible to reduce the treatment volume, thus sparing more normal tissue, without compromising GTV coverage. Improving the quality of life for these patients with poor life expectancy is of great value which makes this adaption a potential candidate for a new protocol for radiotherapy of glioblastoma patients. An alternative would be to add a SIB, since we have shown that this could increase target coverage while still keeping radiation doses to normal tissue lower compared to the original treatment plans. This way of improving tumour control could be one complementary factor for the need of more uncertainty management, due to the use of smaller margins.

Chapter 7

FUTURE ASPECTS

The results of this study implies that it could be reasonable to initiate a clinical trial regarding reducing CTV margins for glioblastoma patients. The major interest of the trial would be whether modifying the treatment volume affects the recurrence pattern and if higher local dose coverage of the GTV really equals better tumor control. Currently an ongoing clinical trial is investigating whether dose-escalation of photon IMRT or proton beam therapy (both with a SIB to 75 Gy/30 fractions) will improve overall survival for glioblastoma patients [41].

Chapter 8

ACKNOWLEDGEMENTS

I would like to start with thanking my supervisors Jonas Scherman, Per Munck af Rosenschöld, Michael Lundemann, Daniel Gasic and Søren Møller. I am grateful to have been blessed with such helpful and supportive supervisors along this journey.

Thank you

- Jonas, for criticizing most things I do in life (especially my choice of socks and pants combination) and your continuous support throughout this project.
- Per, for despite your immensely busy schedule, always managing to make time for me whenever needed.
- Michael and Daniel, for making me feel welcomed at the radiotherapy department in Rigshospitalet and for being my lifelines during the whole dose planning process.
- Sören, for helping me evaluating my treatment plans.

I would also like to extend my gratitudes to Vilberg Jóhannesson, for helping me getting started in Eclipse™, and Per Nilsson, for your valuable inputs regarding some statistical problems.

Bibliography

[1] Cancerfonden. Cancersjukdomarna som drabbar flest [Internet]. Stockholm: Publisher; 2019 [updated 2019-02-11; cited 2019-05-30]. Available from: https://www.cancerfonden.se/om-cancer/cancersjukdomarna-som-drabbar-flest

[2] Stupp R, Mason WP, van den Bent MJ, Weller M, Fisher B, Taphoorn MJB, et al. Radiotherapy plus Concomitant and Adjuvant Temozolomide for Glioblastoma. N Engl J Med 2005; 352:987-996. doi: 10.1056/NEJMoa043330

[3] NORDCAN Association of the Nordic Cancer Registries. Projektet NORDCAN [Internet]. [updated 2019-03-26; cited 2019-05-30]. Available from: http://www-dep.iarc.fr/NORDCAN/SW/frame.asp

[4] Fisher JL, Schwartzbaum JA, Wresch M, Wiemels JL. Epidemiology of brain tumors. Neurol Clin. 2007 Nov;25(4):867-90. doi: 10.1016/j.ncl.2007.07.002

[5] Kirkpatrick JP, Laack NN, Shih H A Gondi V. Management of GBM: a problem of local recurrence. J Neurooncol. 2017 Sep;134(3):487-493. doi: 10.1007/s11060-016-2347-y.

[6] Lundemann M, Costa JC, Law I, Engelholm SA, Muhic A, Poulsen HS, et al. Patterns of failure for patients with glioblastoma following O-(2-[18F]fluoroethyl)-L-tyrosine PET- and MRI-guided radiotherapy. Radiother Oncol. 2017 Mar;122(3):380-386. doi: 10.1016/j.radonc.2017.01.002.

[7] Munck Af Rosenschold P, Law I, Engelholm S, Engelholm SA, Muhic A, Lundemann MJ, et al. Influence of volumetric modulated arc therapy and FET-PET scanning on treatment outcomes for glioblastoma patients. Radiother Oncol. 2019 Jan;130:149-155. doi: 10.1016/j.radonc.2018.10.003.

[8] Baskar R, Dai J, Wenlong N, Yeo R, Yeoh KW. Biological response of cancer cells to radiation treatment. Front Mol Biosci. 2014; 1: 24. doi: 10.3389/fmolb.2014.00024

[9] National Cancer Institute. What Is Cancer? [Internet]. Bethesda, Maryland: National Cancer Institute; 2015 [cited 2019 Feb 1] Available at: https://www.cancer.gov/about-cancer/understanding/what-is-cancer

[10] Davis ME. Glioblastoma: Overview of Disease and Treatment. Clin J Oncol Nurs. 2016 Oct 1; 20(5): S2–S8. doi: 10.1188/16.CJON.S1.2-8

[11] Gupta A Dwivedi T. A Simplified Overview of World Health Organization Classification Update of Central Nervous System Tumors 2016. J Neurosci Rural Pract. 2017 Oct-Dec; 8(4): 629–641. doi: 10.4103/jnrp.jnrp_168_17

[12] Alifieris C Trafalis DT. Glioblastoma multiforme: Pathogenesis and treatment. Pharmacol Ther. 2015 Aug;152:63-82. doi: 10.1016/j.pharmthera.2015.05.005.

[13] Young RM, Jamshidi A, Davis G Sherman JH. Current trends in the surgical management and treatment of adult glioblastoma. Ann Transl Med. 2015 June;3(9). doi: 10.3978/j.issn.2305-5839.2015.05.10

[14] Wen PY, Macdonald DR, Reardon DA, Cloughesy TF, Sorensen AG, Galanis E, et al. Updated response assessment criteria for high-grade gliomas: response assessment in neuro-oncology working group. J Clin Oncol. 2010 Apr 10;28(11):1963-72. doi: 10.1200/JCO.2009.26.3541.

[15] Macdonald DR, Cascino TL, Schold SC Jr and Cairncross JG. Response Criteria for Phase II Studies of Supratenotorial Malignant Glioma. J Clin Oncol. 1990 Jul;8(7):1277-80. doi: 10.1200/JCO.1990.8.7.1277.

[16] Salazar OM Rubin P. The spread of glioblastoma multiforme as a determining factor in the radiation treated volume. Int J Radiat Oncol Biol Phys. 1976: 1(7-8):627–37. doi: doi.org/10.1016/0360-3016(76)90144-9

[17] Jaffray DA Gospodarowicz MK. Cancer: Disease Control Priorities, Third Edition (Volume 3). Washington (DC): The International Bank for Reconstruction and Development / The World Bank; 2015 Nov 1. Chapter 14, Radiation Therapy for Cancer; p. 239-47

[18] InformedHealth.org [Internet]. Cologne, Germany: Institute for Quality and Efficiency in Health Care (IQWiG); 2006-. External radiotherapy. 2007 Dec 21 [Updated 2016 Dec 30]. Available from: https://www.ncbi.nlm.nih.gov/books/NBK279300/

[19] Taylor A Powell MEB. Intensity-modulated radiotherapy—what is it? Cancer Imaging. 2004 Jan;4(2):68–73. DOI: 10.1102/1470-7330.2004.0003

[20] Otto K. Volumetric modulated arc therapy: IMRT in a single gantry arc. Med Phys. 2008 Jan;35(1):310-7. doi: 10.1118/1.2818738.

[21] Katsochi D. Radiation Therapy with a Simultaneous Integrated Boost. In: Onal C, editor. Radiotherapy. IntechOpen. 2017. Available from: https://www.intechopen.com/books/radiotherapy/radiation-therapy-with-a-simultaneous-integrated-boost

[22] ICRU. Prescribing, recording, and reporting photon-beam intensity-modulated radiation therapy (IMRT). Journal of the ICRU Vol 10 No 1 (2010) Report 83. Oxford University Press. doi: 10.1093/jicru/ndq001

[23] Burnet NG, Thomas SJ, Burton KE, Jefferies SJ. Defining the tumour and target volumes for radiotherapy. Cancer Imaging. 2004; 4(2): 153–161. doi: 10.1102/1470-7330.2004.0054

[24] Varian Medical Systems. Eclipse Photon and Electron Instructions for Use. 2014 Sep.

[25] Zhao F, Li M, Kong L, Zhang G Yu J. Delineation of radiation therapy target volumes for patients with postoperative glioblastoma: a review. Onco Targets Ther. 2016; 9: 3197–3204. doi: 10.2147/OTT.S104241

[26] Wernicke AG, Smith AW, Taube S Mehta MP. Glioblastoma: Radiation treatment margins, how small is large enough? Pract Radiat Oncol. 2016 Sep-Oct;6(5):298-305. doi: 10.1016/j.prro.2015.12.002.

[27] Halperin EC, Wazer DE, Brady LW Perez CA. Perez and Brady's principles and practice of radiation oncology. 5 ed. Philadelphia: Lippincott Williams Wilkins; 2017.

[28] Liguori C, Frauenfelder G, Massaroni C, Saccomandi P, Giurazza F, Pitocco F, et al. Emerging clinical applications of computed tomography. Med Devices (Auckl). 2015;8:265–278. doi:10.2147/MDER.S70630

[29] Chu JC, Ni B, Kriz R, Amod Saxena V. Applications of simulator computed tomography number for photon dose calculations during radiotherapy treatment planning. Radiother Oncol. 2000 Apr;55(1):65-73. doi: https://doi.org/10.1016/S0167-8140(00)00159-6

[30] Berger A. How does it work? Positron emission tomography. BMJ. 2003;326(7404):1449. doi:10.1136/bmj.326.7404.1449

[31] Benamor M, Ollivier L, Brisse H, Moulin-Romsee G, Servois V, Neuenschwander S. PET/CT imaging: what radiologists need to know. Cancer Imaging. 2007;7 Spec No A(Special issue A):S95–S99. doi:10.1102/1470-7330.2007.9012

[32] Grover VP, Tognarelli JM, Crossey MM, Cox IJ, Taylor-Robinson SD, McPhail MJ. Magnetic Resonance Imaging: Principles and Techniques: Lessons for Clinicians. J Clin Exp Hepatol. 2015;5(3):246–255. doi:10.1016/j.jceh.2015.08.001

[33] Rees J. Advances in magnetic resonance imaging of brain tumours. Curr Opin Neurol. 2003 Dec;16(6):643-50. doi: 10.1097/01.wco.0000102626.38669.b9

[34] Kathirvel M, Subramanian S, Clivio A, Arun G, Fogliata A, Nicolini G, et al. Critical appraisal of the accuracy of Acuros-XB and Anisotropic Analytical Algorithm compared to measurement and calculations with the compass system in the delivery of RapidArc clinical plans. Radiat Oncol. 2013 Jun 11;8:140. doi: 10.1186/1748-717X-8-140.

[35] Tsien CI, Brown D, Normolle D, Schipper M, Piert M, Junck L, et al. Concurrent temozolomide and dose-escalated intensity-modulated radiation therapy in newly diagnosed glioblastoma. Clin Cancer Res. 2012 Jan 1;18(1):273-9. doi: 10.1158/1078-0432.CCR-11-2073.

[36] Wilcoxon F. Individual Comparisons by Ranking Methods. Biometrics Bulletin. 1945;1(6):80–83. doi: 10.2307/3001968

[37] Fieller EC, Hartley HO, Pearson ES. Tests for rank correlation coefficients. I, Biometrika. 1957;44(3-4):470-481. doi: doi.org/10.1093/biomet/44.3-4.470

[38] Lawrence YR, Li XA, el Naqa I, Hahn CA, Marks LB, Merchant TE and Dicker AP. Radiation dose-volume effects in the brain. Int J Radiat Oncol Biol Phys. 2010 Mar;76(3 Suppl):20-7. doi: 10.1016/j.ijrobp.2009.02.091.

[39] Eriksson PS, Perfilieva E, Björk-Eriksson T, Alborn AM, Nordborg C, Peterson DA Gage FH. Neurogenesis in the adult human hippocampus. Nat Med. 1998 Nov;4(11):1313-7. doi: 10.1038/3305.

[40] Gondi V, Pugh SL, Tome WA, Caine C, Corn B, Kanner A, Rowley H, et al. Preservation of memory with conformal avoidance of the hippocampal neural stem-cell compartment during whole-brain radiotherapy for brain metastases (RTOG 0933): a phase II multi-institutional trial. J Clin Oncol. 2014 Dec 1;32(34):3810-6. doi: 10.1200/JCO.2014.57.2909.

[41] ClinicalTrials.gov. National Library of Medicine (U.S.). (2014, October 27 -). Randomized phase II trial of hypofractionated dose-escalated photon IMRT or proton beam therapy versus conventional photon irradiation with concomitant and adjuvant temozolomide in patients with newly diagnosed glioblastoma. Identifier NCT02179086. Retrieved May 31, 2019 from: https://clinicaltrials.gov/ct2/show/NCT02179086?term=NCT02179086.rank=1

Appendix A

Identity plots

A.1 New treatment plan vs. original treatment plan

The plots below represent a comparison of simulated doses to different treatment target structures and OARs between the new (1 cm CTV margin) and original (2 cm CTV margin) treatment plans. All doses are presented as absolute doses, in Gray. Identity lines are shown in blue. Pay attention to the scales of the axes.

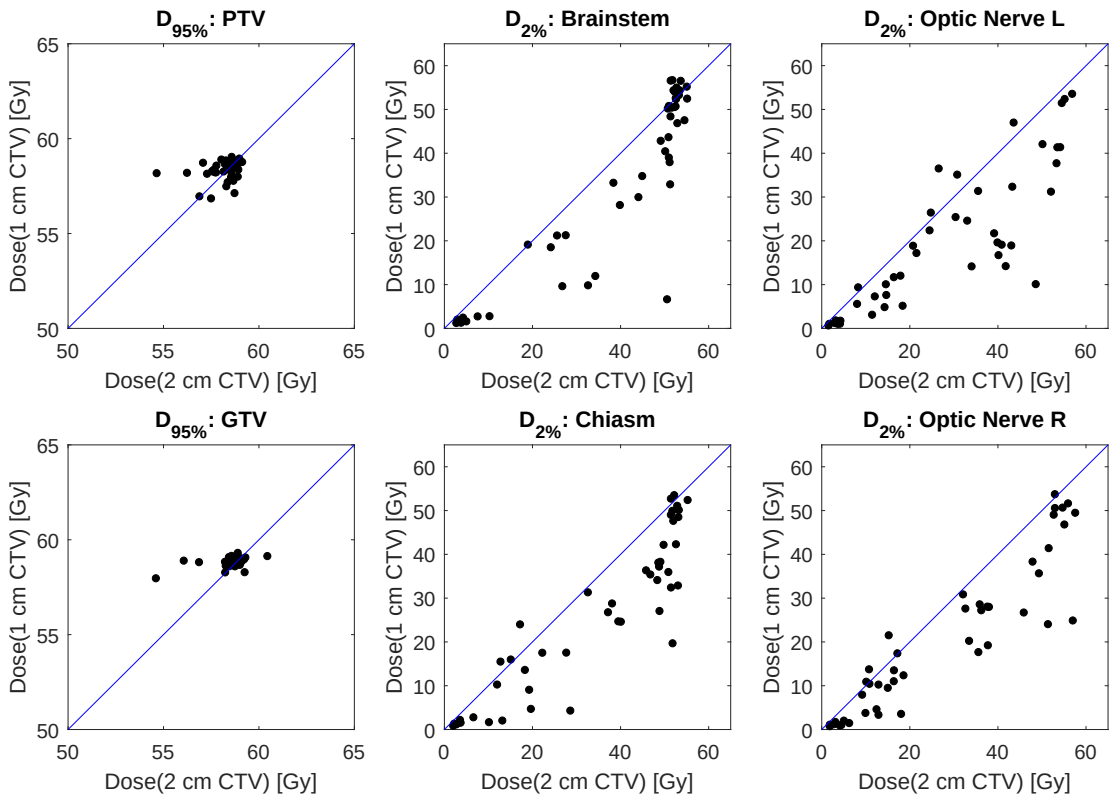

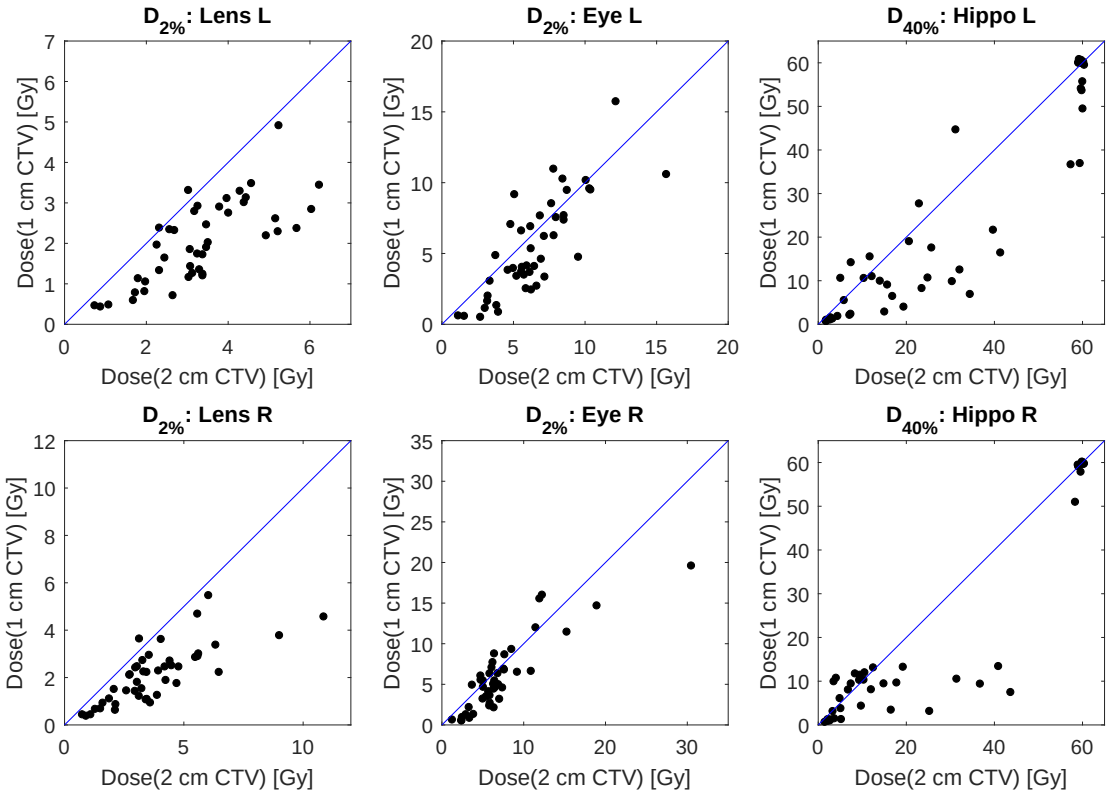

A.2 Reducing CTV margins combined with SIB

The plots below represent a comparison of simulated doses to different treatment target structures and OARs between the new SIB-plans and original (2 cm CTV margin) treatment plans. All doses are presented as absolute doses, in Gray. Identity lines are shown in blue.

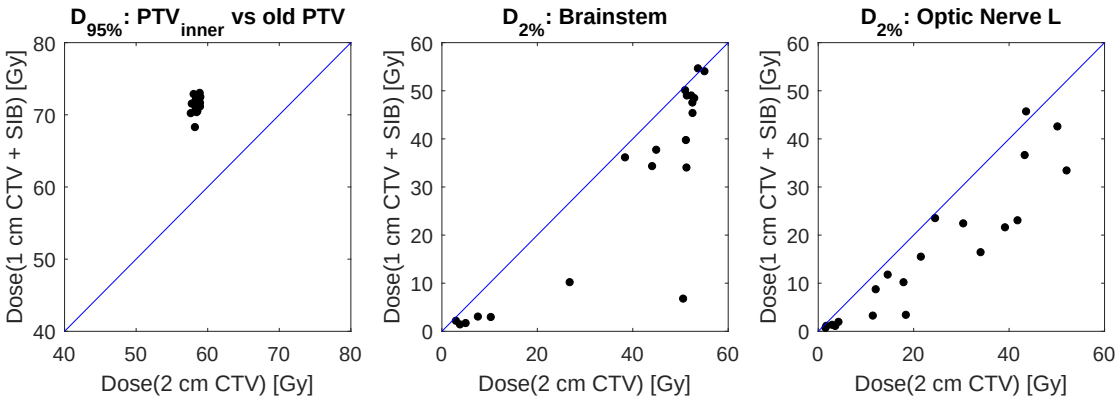

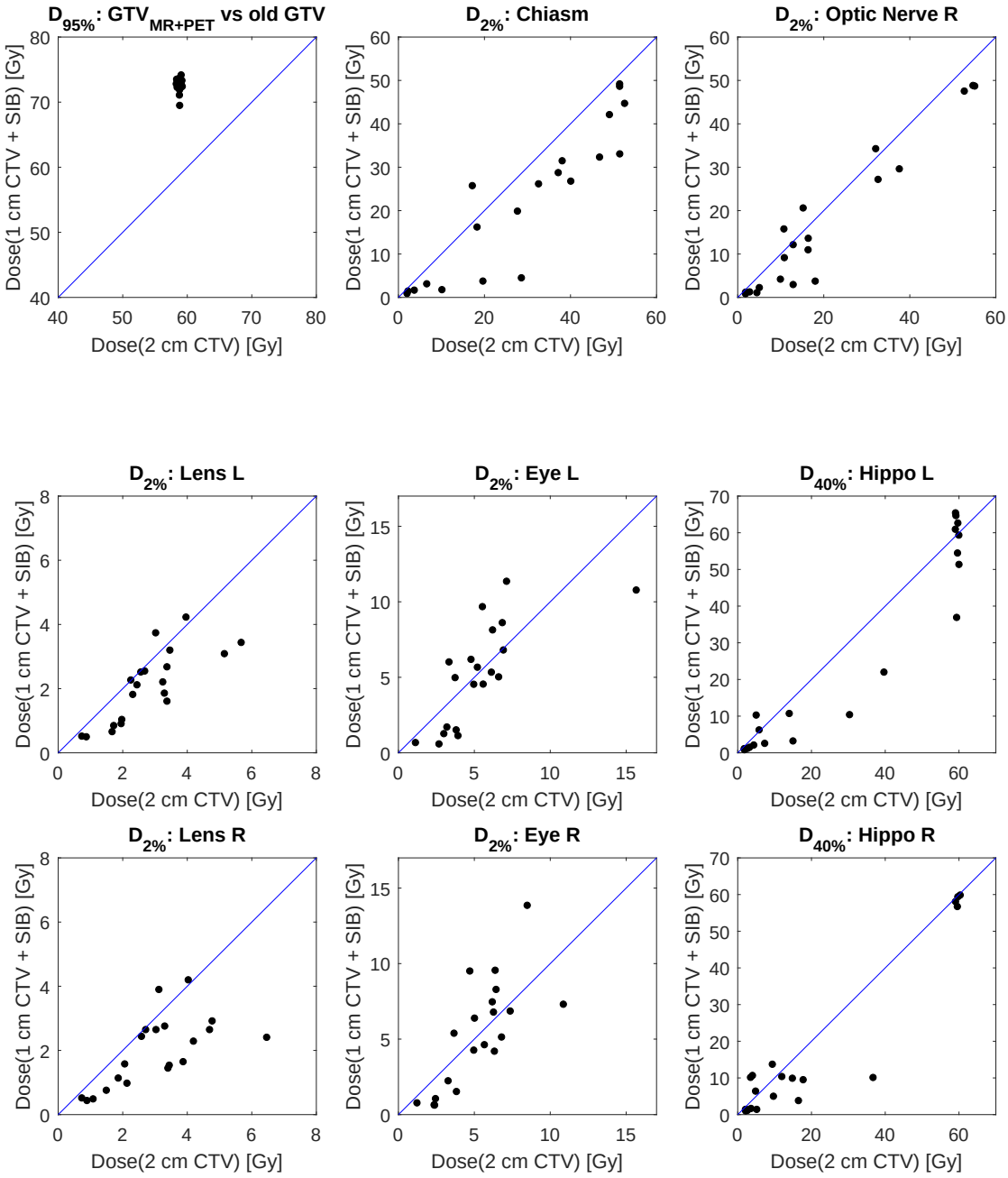
D95%: GTVMR+PET vs old GTV
D2%: Chiasm
D2%: Optic Nerve R
D2%: Lens L
D2%: Eye L
D40%: Hippo L
D2%: Lens R
D2%: Eye R
D40%: Hippo R
Dose(1 cm CTV + SIB) [Gy]
Dose(2 cm CTV) [Gy]

A.3 Acuros-XB vs. AAA

The plots below represent a comparison of simulated doses to different treatment target structures and OAR's between treatment plans optimized and calculated with dose calculation algorithms Acuros-XB and AAA. All doses are presented as absolute doses, in Gray. Identity lines are shown in blue.

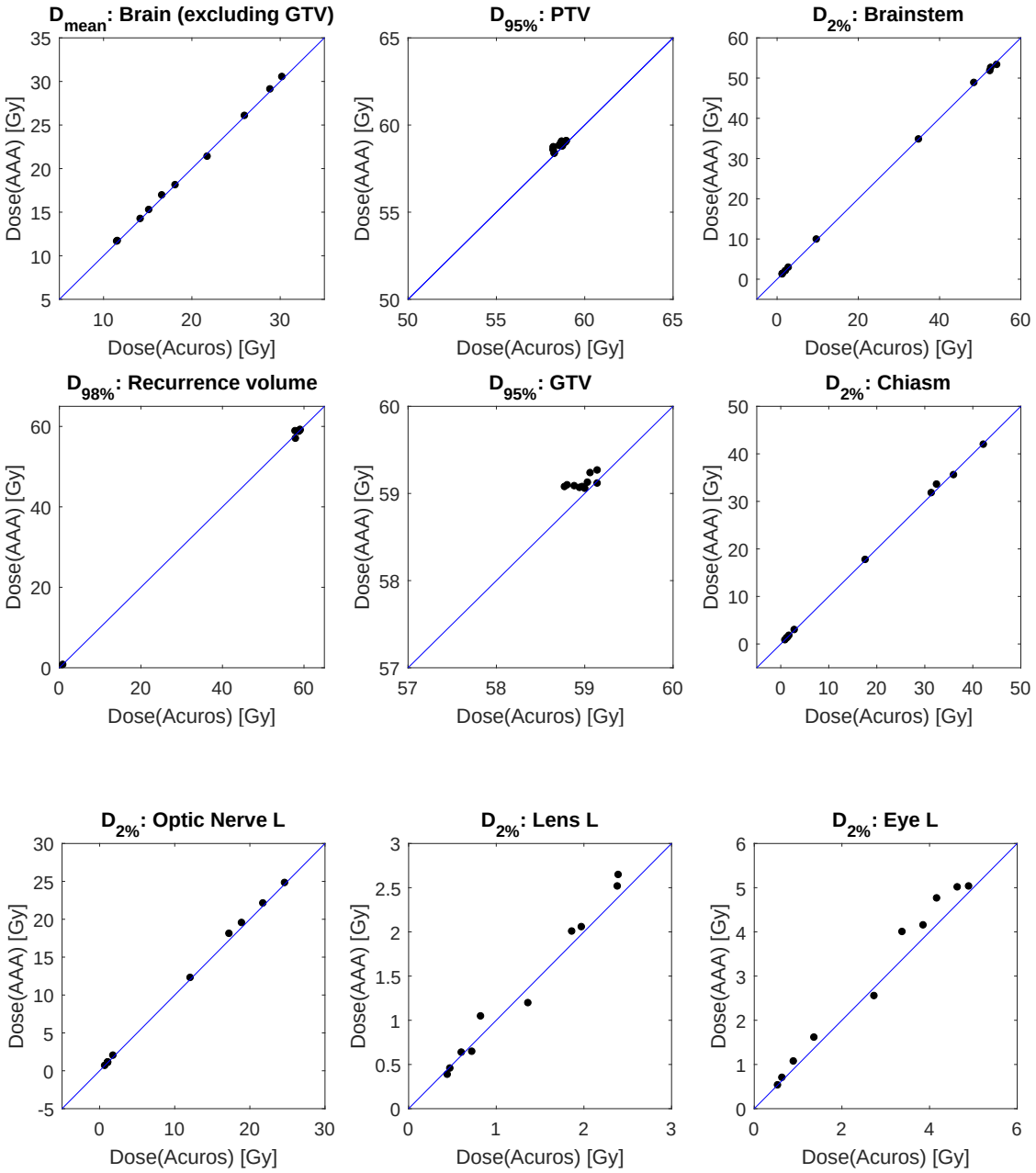

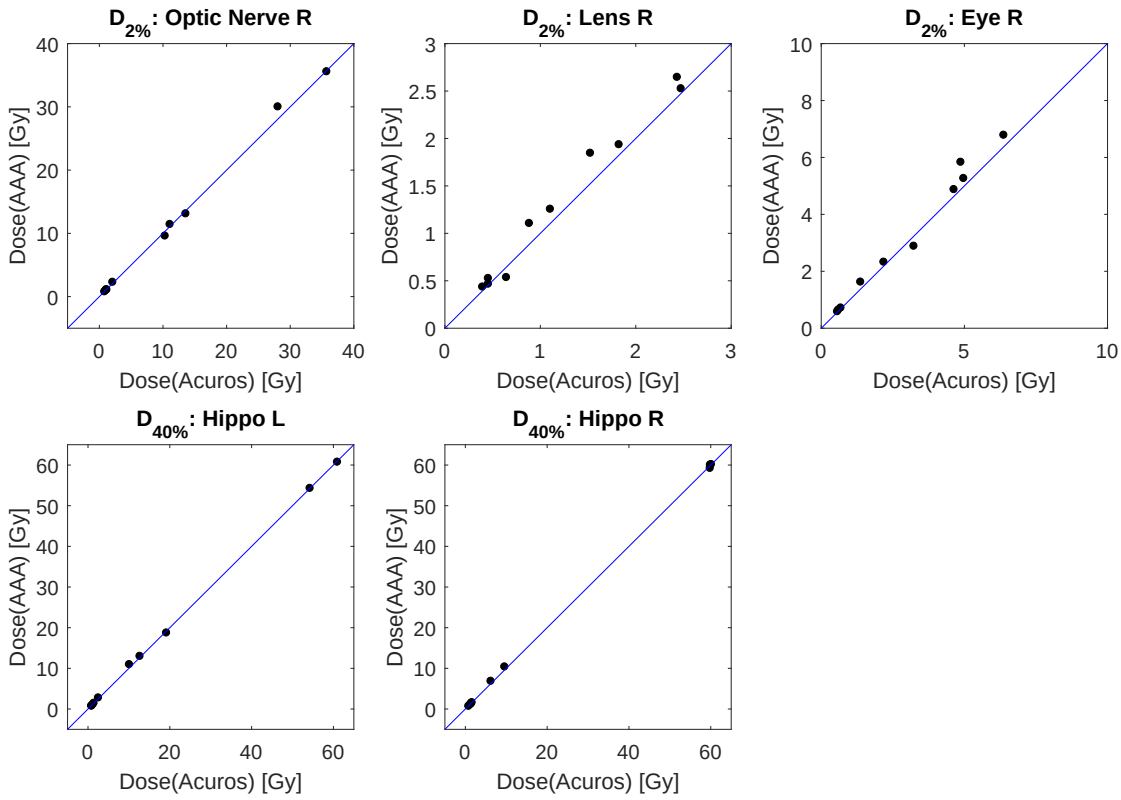
D2%: Optic Nerve R
Dose(AAA) [Gy]
Dose(Acuros) [Gy]
D2%: Lens R
Dose(AAA) [Gy]
Dose(Acuros) [Gy]
D2%: Eye R
Dose(AAA) [Gy]
Dose(Acuros) [Gy]
D40%: Hippo L
Dose(AAA) [Gy]
Dose(Acuros) [Gy]
D40%: Hippo R
Dose(AAA) [Gy]
Dose(Acuros) [Gy]